A WAVELET APPROACH ON NM IMAGES FILTERING USING ADJACENT IMAGES INFORMATION

Cvetko D. Mitrovski, Ph.D., Mitko B. Kostov, M.Sc.

University St. Kliment Ohridski, Faculty of Technical Sciences, Bitola – Macedonia,
cvetko.mitrovski@uklo.edu.mk, mitko.kostov@uklo.edu.mk

Abstract – **In this paper we present our approach on pre-processing chest region dynamic NM images. It enables anatomical data extraction of the vena cava and the heart. The aim of the method is developing sophisticated diagnostic software that could automatically offer the optimal positions and the shapes of the regions of interest needed for heart studies.**

Key words **Nuclear medicine image, wavelet-domain filtering, autocorrelation, denoising.**

1. INTRODUCTION

Nuclear Medicine (NM) images are diagnostic digital images, which provide both anatomical and functional information. They present the projection of the distribution of radioisotope(s) in a body of a patient after injection of adequate dose of radioisotope(s). The raw NM images are created by accumulating the emitted gamma rays from a patient over a fixed observation period by computerized gamma cameras. They have a low signal-to-noise ratio (SNR) due to the nature of the gamma ray emission process and the operational characteristics of the gamma cameras (low count levels, scatter, attenuation, and electronic noises in the detector/camera). The noise obeys a Poisson law and is highly dependent on the space distribution of the image signal intensity. Therefore, a suitable image pre-processing must precede the NM images analysis in order to provide an accurate recognition of the anatomical data of the patient (the boundaries of the various objects – organs). This process of separating signal from noise is a rather difficult and much diversified task that should be adjusted to the organs and tissues, which physiology is to be investigated.

In [1], [2], [3], [4] and [5] we proposed several approaches to cope with this problem. In [1] the whole process of spreading of the radionuclide is divided in three successive phases and the images that belong to one specific phase are processed separately from the others. The processing includes changing images resolution and applying autocorrelation technique. In [2] the images are filtered by applying the wavelet shrinkage program, where the set threshold is same for all the wavelet coefficients in one level. In [3] the images' denoising is carried out by modifying images histogram. In [4] we try to denoise images by filtering in the direction that is normal to the radionuclide spreading direction. In [5] we combine DWT realized via QMF filters with a specific strategy for selecting an appropriate threshold. Due to the signal-dependence of the Poisson noise, the Anscombe variance-stabilizing transformation is applied.

This paper presents a new approach on pre-processing of NM heart-region images. The images are processed in the discrete wavelet transform domain with linear phase QMF filters. The filters are designed to achieve both good image decomposition and near perfect reconstruction. Information from adjacent images is used while filtering particular image.

The paper is organized as follows. In Section II the NM images creation process is modelled, and the problems due which raw NM images should be pre-processed, are formulated. The wavelet theory and wavelet-domain filtering are reviewed in Section 3. In Section 4 we propose a suitable chest-region NM images filtration technique where we use the information from neighbourhood images. The performance of the approach is demonstrated on real NM images in Section 5, while the conclusion is given in Section 6.

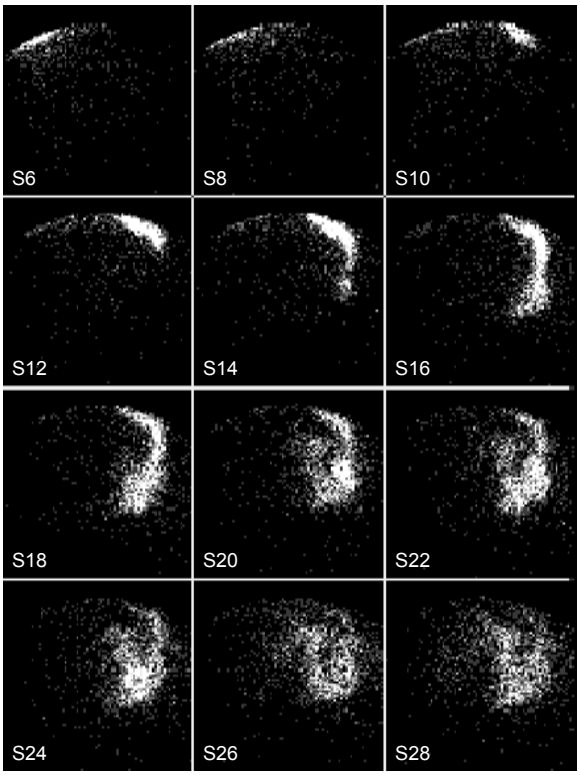

Fig. 1 Sequence of enhanced noised images (τ=0.4 s)

2. NM IMAGE CREATION PROCESS

The process of generating the NM images starts after injection of certain, small dose (for safety reasons) of suitably chosen radioactive material, into the body of a patient. The radionuclide spreads and mixes with the blood on its way to the heart through the vena cava superior. This results with some very complicated, fast changing function, $\rho(x, y, z, t)$. After passing through the heart, the blood-radioactivity mixture passes through the lungs, returns to the heart and proceeds with spreading toward each cell of the patient body through its arteries. This process could be recorded as a set of *N*, NM images (Fig. 1). Each image contains rather high level of noise caused by: a) mixing the radionuclide with the blood and the spreading of this mixture, b) hydrodynamic processes in the blood vessels caused by the pumping work of the heart, and c) by the randomness of the gamma rays emission and their detection by the gamma camera. Considering this, the raw images should be adequately pre-processed in order to extract the anatomy information about the position of the vena cava superior and the heart. According to this information, the optimal position (and the shape) of the regions of interest (ROI's) for the heart study could be proposed [7].

3. AN OVERVIEW OF THE DISCRETE WAVELET TRANSFORM

The Discrete Wavelet Transform (DWT) decomposes a signal into a set of orthogonal components describing the signal variation across the scale [7]. The orthogonal components are generated by dilations and translations of a prototype function ψ called *mother wavelet.*

$$\psi_{i,k}(t) = 2^{-i/2}\psi(t/2^i - k), \quad k, i \in Z \tag{1}$$

The above equation shows that the mother function is dilated by the integer *i* and translated by the integer *k*. In analogy with other function expansions, a function *f* may be written for each discrete coordinate *t* as sum of a wavelet expansion up to certain scale *J* plus a residual term, that is:

$$f(t) = \sum_{j=1}^{J} \sum_{k=1}^{2^{-j}M} d_{jk}\psi_{jk}(t) + \sum_{k=1}^{2^{-J}M} c_{Jk}\phi_{Jk}(t) \tag{2}$$

The estimation of d_{jk} and c_{Jk} is carried out through an

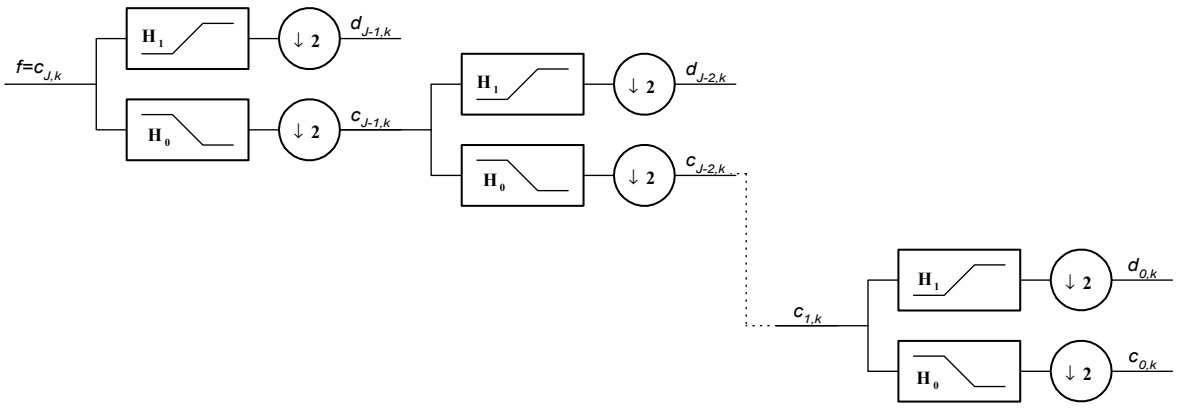

Fig. 2. Discrete Wavelet Transform Tree

iterative decomposition algorithm, which uses two complementary filters h_0 (low-pass) and h_1 (high-pass). Since the wavelet base is orthogonal, h_0 and h_1 satisfies the quadrature mirror filter conditions (QMF) [12]. Filter bank theory is closely related to wavelet decompositions and multiresolution concepts. For this reason, it is helpful at this point to view the scaling function ϕ as a low pass filter h_0 and the wavelet function ψ as a high pass filter h_1. The mother and scaling functions are defined as follows [8]:

$$\psi(t) = \sum_n 2^{1/2} h_1 \psi(2t - n) \tag{3}$$

$$\phi(t) = \sum_n 2^{1/2} h_0 \phi(2t - n) \tag{4}$$

For computation of wavelet transform, the following pyramidal algorithm is used: The QMF bank decomposes the signal into low and high frequency components respectively. Convolving the signal with h_1 gives a set of wavelet coefficients $c_{J,k}$, while the convolution with h_0 gives the approximation coefficients $d_{j,\mathrm{k}}$. Because of the redundancy of information, these filters are down-sampled, throwing away every other sample at each operation, thus halving the data each time. The approximation coefficients $d_{j,k}$ are then convolved again with the filters h_0 and h_1 to form the next level of decomposition. The backward algorithm simply inverts the process. It combines two linear filters with up-sampling operation. Fig. 2 shows the operation involved in the wavelet decomposition and synthesis of the signal.

At present, there exist no theoretical results that can predict which wavelet is suitable for a particular type of signal. Usually, the best wavelet is chosen by comparing the performances of several types of wavelets.

Wavelet Shrinkage

The most popular form of wavelet-based filtering is commonly known as *Wavelet Shrinkage*. The basic wavelet shrinkage algorithm involves computing of the discrete wavelet transform of the observation y (w = DWT(y)). The contribution of a particular wavelet basis function in the signal expansion can be filtered by weighting the corresponding coefficient w_i by a number $0 \le h_i \le 1$. That is, the wavelet coefficients are modified according to:

$$\hat{w}_i = w_i \cdot h_i \tag{5}$$

In the wavelet shrinkage program, the shrinkage filter corresponds to either the "hard threshold" nonlinearity

$$h_i^{(\mathrm{hard})} = \begin{cases} 1, & \text{if } |w_i| \ge \tau \\ 0, & \text{if } |w_i| < \tau \end{cases} \tag{6}$$

or the "soft threshold" nonlinearity

$$h_i^{(\mathrm{soft})} = \begin{cases} 1 - \dfrac{\tau \operatorname{sgn}(w_i)}{w_i}, & \text{if } |w_i| \ge \tau \\ 0, & \text{if } |w_i| < \tau \end{cases} \tag{7}$$

with τ a user-specified threshold level.

Finally, the signal is reconstructed (estimated) by computing the inverse wavelet transform from the processed data: $\hat{f}$ = IDWT($\hat{w}$).

4. FILTRATION OF DYNAMIC NM IMAGES

The heart region images contain quantum noise that obeys Poisson law and is highly dependent on the underlying light intensity pattern being imaged [9]. For denoising purposes, it is often advantageous instead of working in the spatial (pixel) domain to work in a transform domain. One possible choice for images transform is the discrete wavelet transform (DWT) domain. The DWT tends to concentrate the energy of a signal into a small number of coefficients, while a large number of coefficients have low SNR.

Motivated by the DWT tendency to produce coefficients with a high and low SNR, we apply the soft thresholding from the wavelet shrinkage program.

Moreover, the wavelet shrinkage program implies discarding some of the wavelet coefficients, so the signal perfect reconstruction is not possible. Hence, we propose to give up the perfect reconstruction at the very beginning. It means instead to use wavelet filters, to decompose the data using a filter bank with filters that have better characteristics. At the same time, we design the QMF bank to achieve near perfect reconstruction (NPR). One possible choice to design a QMF NPR bank is to use the algorithm proposed in [10].

Since the dynamic images are consecutive, it can be expected that each image contains information that can be used for filtering of its adjacent images. In order to use this information we form MxN vectors by joining all the pixels from all the images that are located at same position, where MxN is the resolution of the images (Fig. 3-a). The vectors have length K, where K is the total number of images in the images set. One

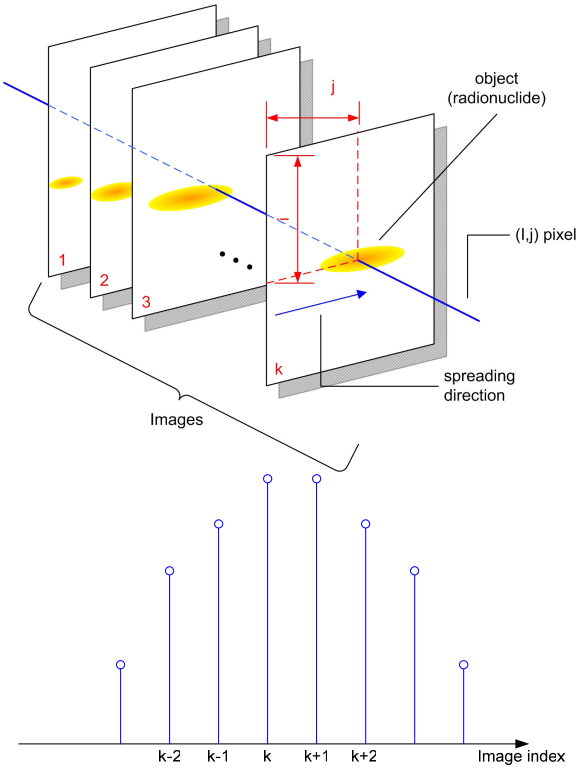

Fig. 3 a) Set of NM images; b) Expected shape of a vector created by joining the pixels from all the images that are located at same position

can expect that when images do not contain noise the created vectors should form a shape similar to that given in Fig. 3-b. However, the vectors obtained from real NM images form a shape given in Fig 4. The isolated peaks in Fig. 4 are result of the noise presence in the images. In order to eliminate these peaks we propose to do wavelet filtering to all of these vectors.

Eventually, we summarize the algorithm for denoising chest region images as follows:

- apply autocorrelation technique to each image separately [1];
- compute 2D DWT of each image using a QMF NPR bank;
- apply the standard soft-thresholding to the wavelet coefficients of each image;
- compute inverse DWT using modified wavelet coefficients;
- create vectors by joining the pixels from all the images that are located at same position;
- compute 1D DWT of each vector at level 1;
- compute inverse DWT using only the approximation coefficients;
- form images from the modified vectors;
- form the resultant image from the filtrated images.

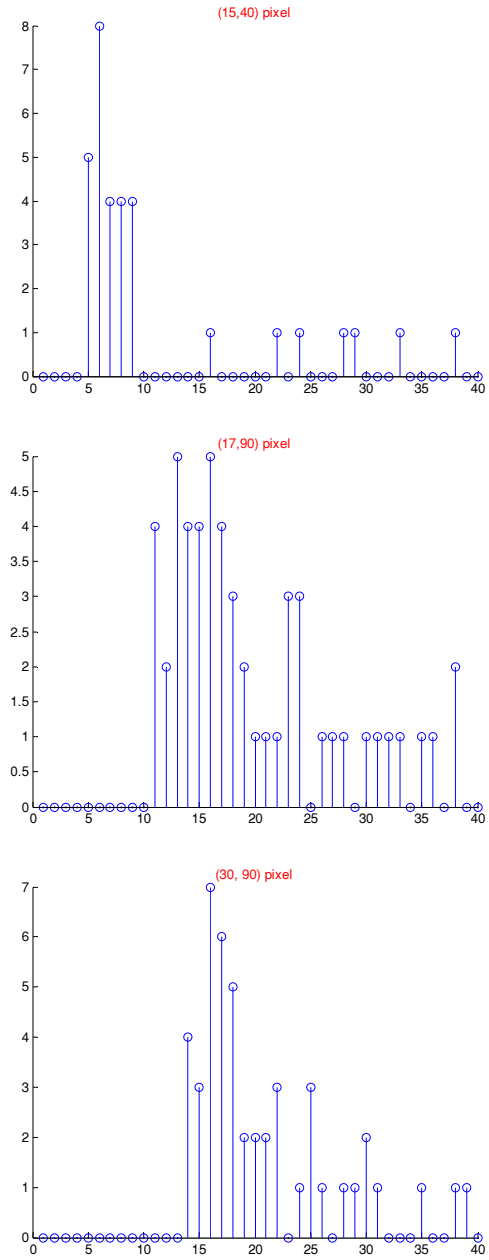

Fig. 4 Vectors created from the pixels at same position in the raw NM images

5. EXPERIMENTAL RESULTS

In this Section, we illustrate the effects of applying our method and compare these effects with the results obtained by using the conventional approach. Both methods were applied on a same subset of 24 sequential dynamic NM images (Fig. 1), recorded with resolution 128x128 and accumulation time τ=0.4 [s].

To design suitable QMF NPR bank needed for computing 2D DWT we used the algorithm described

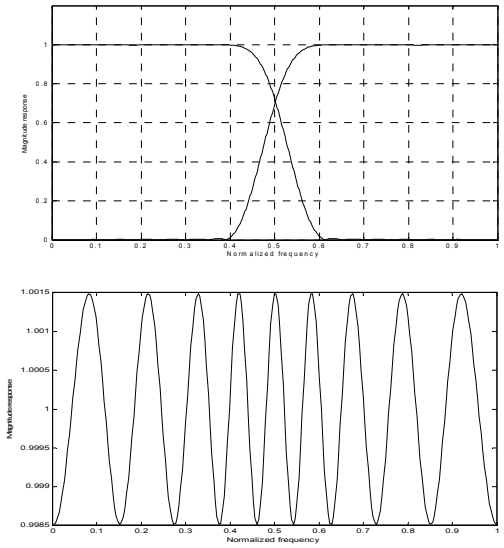

Fig. 5 a) Magnitude responses of the decomposing filters, b) Magnitude response of the QMF NPR bank

Table 1 Filter coefficients of QMF bank filters

$h_0[0–15] = h_0[31–16]$	0.002722 -0.002856 -0.003194 0.007698 0.002690 -0.015823 0.000046 0.027907 -0.007397 -0.046104 0.023106 0.075651 -0.058667 -0.140412 0.184563 0.657174
$h_1[0–15]= –h_1[31–16]$	0.002722 0.002856 -0.003194 -0.007698 0.002690 0.015823 0.000046 -0.027907 -0.007397 0.046104 0.023106 -0.075651 -0.058667 0.140412 -0.184563 -0.657174
$f_0[0–15] = f_0[31–16]$	0.002722 -0.002856 -0.003194 0.007698 0.002690 -0.015823 0.000046 0.027907 -0.007397 -0.046104 0.023106 0.075651 -0.058667 -0.140412 0.184563 0.657174
$f_1[0–15] = –f_1[31–16]$	-0.002722 -0.002856 0.003194 0.007698 -0.002690 -0.015823 -0.000046 0.027907 0.007397 -0.046104 -0.023106 0.075651 0.058667 -0.140412 -0.184563 0.657174

in [10]. The designed QMF bank has overall reconstruction error minimized in the minimax sense; the corresponding QMF filters have least-squares stopband error. The filters have linear phase, zero at π, good passband and narrow transition band. The decomposition filters magnitude response and the prototype filter coefficients are given in Fig. 5 and Table 1, respectively.

The effect of use of 1D wavelet filtering to the vectors created by joining the pixels located at a same position in raw NM images is shown in Fig. 6. In order effect to be easily noticed, Fig. 6 illustrates the effect of 1D wavelet filtering to raw NM images, not to images firstly filtered with autocorrelation technique and 2D wavelet filtering. In view of the used filters, we decomposed the vectors by using the wavelet db3 and reconstructed them by using the same wavelet only from the approximation coefficients at level 1. It can

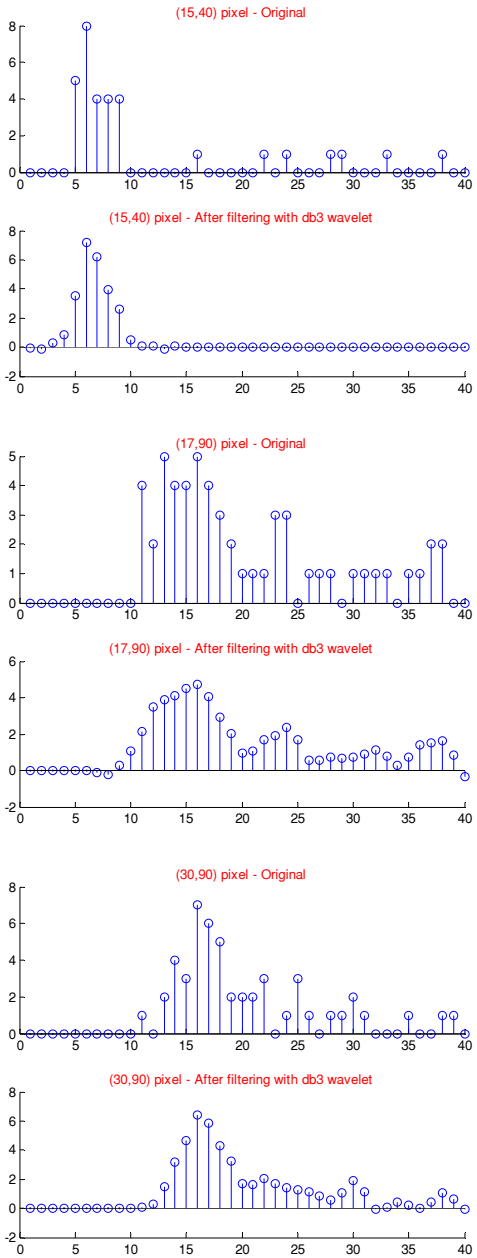

Fig. 6 The effect of using wavelet filtering with db3 to the 1D vectors created from raw NM images

be noticed from Fig. 6 that after processing there is no abrupt changes in the peaks.

The final effect of the proposed method is presented in Fig. 7-a, while the effect of the conventional approach is presented in Fig. 7-b. In the resultant image (Fig. 7-a) the shadow (pixels with low intensity) is removed. This image has sharp edges of the vein and the heart, while the image in Fig. 7-b contains relatively high level of noise that blurs the edges of these objects. Therefore, the image in Fig. 7-a is more suitable for an upgrading expert system that could provide automatic identification of optimal shapes and

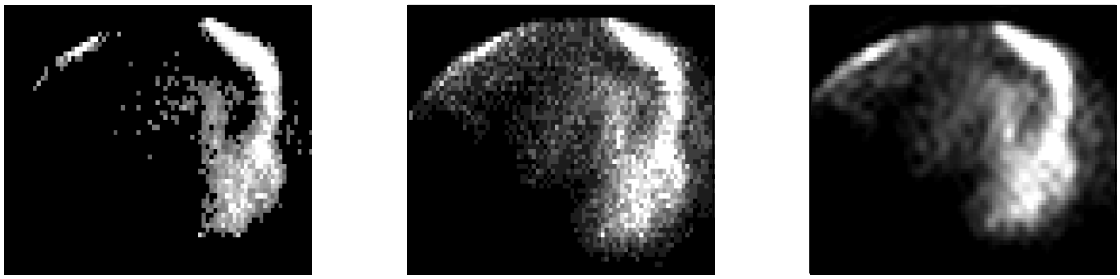

Fig. 7 The vena and the heart a) proposed approach b) conventional approach c) lowpass filtering of the image in b)

positions of regions of interest needed for further physiological diagnostics.

The quality of the image in Fig. 7-b could be further improved by using certain low pass filtering techniques as shown in Fig. 7-c, but the projections of the vein and the heart would still suffer from certain deformations. These deformations could degrade the effects of an expert system for automatic identification of the optimal positions and shapes of regions of interest needed for further investigations.

6. CONCLUSION

We present an approach on pre-processing chest region dynamical NM images. The aim of this approach is to determine anatomical data in order to upgrade the software with an expert system that could identify the optimal positions and the shapes of the regions of interest needed for the heart study. We demonstrate the performance of the proposed method on real dynamical NM images, recorded and processed by our own upgraded gamma camera system developed at the department of NM in Bitola.

7. REFERENCES

[1] Cvetko D. Mitrovski and Mitko B. Kostov, "On the Preprocessing of Dynamic Nuclear Medicine Images", *International Scientific Conference on Information, Communication and Energy Systems and Technologies ICEST 2002*, Nis, Serbia and Montenegro, 2002;

[2] Cvetko D. Mitrovski and Mitko B. Kostov, "A Wavelet Domain Approach On Noise Filtration Of Nuclear Medicine Images", *International Scientific And Applied Science Conference Electronics ET'2002*, Sozopol, Bulgaria, Sept. 2002;

[3] Cvetko D. Mitrovski and Mitko B. Kostov, "An Approach For Extracting The Vein And Heart Boundaries From Raw NM Images", *VI National Conference ETAI 2003*, Ohrid, Macedonia, Sept. 2003;

[4] Cvetko D. Mitrovski and Mitko B. Kostov, "On The Radionuclide Movement Depended Filtering Of Nuclear Medicine Images", *Fourth International Conference for Informatics and Information Technology 2003*, Molika, Macedonia, Dec. 2003;

[5] Mitko B. Kostov and Cvetko D. Mitrovski, "On The Denoising Of Nuclear Medicine Chest Region Images", *International Scientific And Applied Science Conference Electronics ET'2004*, Sozopol, Bulgaria, 22-24 Sept. 2004;

[6] Cvetko D. Mitrovski and Mitko B. Kostov, "QMF Filtering Of Nuclear Medicine Heart Region Images", *International Scientific Conference on Information, Communication and Energy Systems and Technologies ICEST 2005*, Nis, Serbia and Montenegro, 2005;

[7] Cvetko D. Mitrovski, "Quantitative Determination of Left-Right Shunt at Heart Disease Patients", *Proceeding of papers,* Faculty of Technical Sciences – Bitola, pp. 327-335, 1996;

[8] G. Strang and T. Nguyen, *Wavelets and Filter Bank*s. Wellesley-Cambrige Press, 1996;

[9] Robert D. Nowak, Richard G. Baraniuk, "Wavelet-Domain Filtering for Photon Imaging Systems", *IEEE Trans. Image Processing*, vol. 8, Iss. 5, p. 666-678, May 1999;

[10] Sofija Bogdanova, Mitko Kostov, and Momcilo Bogdanov, "Design of QMF Banks with Reduced Number of Iterations", *IEEE Int. Conf. on Signal Processing, Application and Technology, ICSPAT '99,* Orlando, USA, Nov. 1999;

[11] D. L. Donoho, "Wavelet Thresholding and W.V.D.: A 10-minute Tour", *Int. Conf. on Wavelets and Applications*, Toulouse, France, June 1992;

[12] D. L. Donoho and I. M. Johnstone, "Ideal Spatial Adaptation via Wavelet Thresholding", *Biometrika*, vol. 81, pp. 425-455, 1994.